# Canards in $\mathbb{R}^3$

Peter Szmolyan[1] and Martin Wechselberger[1]

*Institut für Angewandte und Numerische Mathematik, TU-Wien,
Wiedner Hauptstr. 8–10, Wien A-1040, Austria*

We give a geometric analysis of canard solutions in three-dimensional singularly perturbed systems with a folded two-dimensional critical manifold. By analysing the reduced flow we obtain singular canard solutions passing through a singularity on the fold-curve. We classify these singularities, called canard points, as folded saddles, folded nodes, and folded saddle-nodes. We prove the existence of canard

## 1. INTRODUCTION

We consider three-dimensional systems of singularly perturbed ordinary differential equations in standard form

$$\begin{aligned}
\dot{x} &= g_1(x, y, z, \varepsilon) \\
\dot{y} &= g_2(x, y, z, \varepsilon) \\
\varepsilon \dot{z} &= f(x, y, z, \varepsilon),
\end{aligned}$$

(1)

with sufficiently smooth functions $g_1$, $g_2$, $f$ and small parameter $0 < \varepsilon \ll 1$. The variables $(x, y) \in \mathbb{R}^2$ are slow variables; $z \in \mathbb{R}$ is a fast variable. The independent variable is the slow time $\tau$.

Properties of solutions of system (1) can be studied by using methods from dynamical systems theory. In the following we present a brief introduction to this approach which is known as *geometric singular perturbation*

*theory*. By transforming from the slow time scale $\tau$ to the fast time scale $t := \tau/\varepsilon$ one obtains the equivalent fast system

$$
\begin{aligned}
x' &= \varepsilon g_1(x, y, z, \varepsilon) \\
y' &= \varepsilon g_2(x, y, z, \varepsilon) \\
z' &= f(x, y, z, \varepsilon)
\end{aligned}
$$
(2)

One tries to analyse the dynamics of system (1) by suitably combining the dynamics of the *reduced problem*

$$
\begin{aligned}
\dot{x} &= g_1(x, y, z, 0) \\
\dot{y} &= g_2(x, y, z, 0) \\
0 &= f(x, y, z, 0)
\end{aligned}
$$
(3)

and the dynamics of the *layer problem*

$$
\begin{aligned}
x' &= 0 \\
y' &= 0 \\
z' &= f(x, y, z, 0),
\end{aligned}
$$
(4)

which are the limiting problems for $\varepsilon = 0$ on the slow and fast time scales, respectively. The foundation of the geometric approach to singular perturbation theory was given by Fenichel [Fen79]. The basic reasoning is as follows. The reduced problem is a dynamical system on the set $S := \{(x, y, z) \in \mathbb{R}^3 : f(x, y, z, 0) = 0\}$. In the following we refer to $S$ as the *critical manifold*. The stability of points $(x, y, z) \in S$ as equilibria of the layer problem (4) depends on the sign of $\partial f / \partial z$. If $\partial f / \partial z\,(x, y, z, 0)$ is uniformly bounded away from zero for all $(x, y, z) \in S_0$, where $S_0 \subset S$ is compact, the critical manifold $S_0$ is normally hyperbolic (see, e.g., [Fen71, HPS77]). Such a normally hyperbolic invariant manifold of equilibria of the layer problem (4) persists as a locally invariant slow manifold $S_\varepsilon$ of the full problem (1) for $\varepsilon$ sufficiently small. The restriction of the flow (1) to $S_\varepsilon$ is a small smooth perturbation of the flow of the reduced problem (3) [Fen79]. For an excellent introduction to geometric singular perturbation theory and an overview of applications we refer to the survey by Jones [Jon95].

For normally hyperbolic critical manifolds the geometric theory is fairly complete. However, this theory breaks down in the neighbourhood of points where normal hyperbolicity is lost, e.g., near bifurcation points of $S$.

The most common situations where this happens are fold points or points of self-intersection of the critical manifold $S$.

The best known class of such problems are *regular folds*, where a jumping behaviour of solutions occurs. The reduced flow is directed towards (or away from) the fold-curve on both branches of the critical manifold. The only possibility for solutions reaching the fold-curve is to jump to another branch of the critical manifold. This process may occur repeatedly as in the well known relaxation oscillations. Classical results by means of matched asymptotic expansions for regular folds can be found in [MR80].

In this paper we focus on the phenomenon of *canards* which is also due to the loss of normal hyperbolicity. A canard solution is a solution of a singularly perturbed system which follows an attracting slow manifold, passes close to a bifurcation point of the critical manifold and then follows, rather surprisingly, a repelling slow manifold for a considerable amount of time. In geometric terms a canard solution corresponds to the intersection of an attracting and a repelling slow manifold near a non-hyperbolic point of $S$. In this context the non-uniqueness of the (center-like) slow manifolds is of some relevance. Sometimes it is advantageous to make a fixed choice of the in general non-unique slow manifolds and then to discuss their intersections. We call the intersection of these fixed slow manifolds a *maximal canard*. Then, canards as described above are orbits (lying in some other slow manifold) exponentially close to the maximal canard.

We will encounter also solutions starting in a repelling slow manifold and ending in an attracting slow manifold. Following the terminology of Benoit [Ben83] we call such solutions *faux canards*. Clearly, the existence of faux canards is less surprising than the existence of canards.

Canard solutions were discovered and first analysed by Benoit, Callot, F. Diener, and M. Diener [BCDD81, Die84, Die94]. They also discovered the phenomenon of *canard explosion*, which denotes a very fast transition upon variation of a parameter from a small amplitude limit cycle via *canard cycles* to a relaxation oscillation. For a treatment of canard cycles by means of matched asymptotic expansions we refer to [Eck83, MKKR94].

A breakthrough in geometric theory came with the work of Dumortier and Roussarie [DR96]. They give a detailed geometric explanation and proof of canard cycles in van der Pol's equation by using blow-up of singularities and foliation by center manifolds as main techniques. The method is very powerful, but also quite intricate. For an introduction to blow-up methods we refer to [Dum91, Dum93].

Inspired by their work Krupa and the first author have recently developed a variant of the blow-up method in the context of singular perturbation problems which draws more on the existing geometric singular perturbation theory. In a series of papers [KS01a, KS01b, KS01c, KS01d] folds, canard

points, relaxation oscillations and canard explosion, and exchange of stability of slow manifolds near transcritical and pitchfork bifurcations of the critical manifold are analysed.

Most of the above results are for planar systems or for systems which can be reduced to them. As far as canards are concerned one has to keep in mind that the planar case is degenerate and canards can occur persistently only in one-parameter families of planar vector fields.

In this paper we continue the geometric analysis of folded critical manifolds for system (2). The *regular fold* case is treated in [Wec98, SW99], where a jumping behaviour of solutions near the fold-curve occurs. This behaviour is very similar to the regular fold in planar systems and our results can be viewed as extensions of the planar case given in [KS01a, KS01b]. Classical results by means of matched asymptotic expansions can be found in [MR80]. Note that regular fold points occur on open segments of the fold-curve. We will see that canards are possible at more degenerate singularities on the fold-curve.

EXAMPLE 1.1. As a motivation consider the following example which is a special case of examples considered in [Ben83]:

$$\dot{x} = -2y$$
(5)
$$\dot{y} = 1$$
$$\varepsilon \dot{z} = x + z^2.$$

The $y$-axis divides the critical manifold $x + z^2 = 0$ into two branches, where the lower one is attracting while the upper one is repelling. Away from the fold-curve the branches of the critical manifold perturb smoothly to slow manifolds. These slow manifolds can be extended by the flow near the fold-curve, but their behaviour is not controlled by the existing hyperbolic theory. Nevertheless there exist two exact solutions of this system given by $(x(t), y(t), z(t)) = (-t^2 \pm \varepsilon, t, \pm t)$, $t \in \mathbb{R}$, which have algebraic growth and hence lie in the slow manifolds for $|t|$ large. For $\varepsilon = 0$ these two solutions correspond to solutions of the reduced flow on the critical manifold $x + z^2 = 0$ passing through the origin from the attracting to the repelling manifold or vice versa (see Fig. 1). Hence, these $\varepsilon = 0$ solutions are *singular canards*. We call the origin a *canard point*. From the exact solutions for $\varepsilon \neq 0$ we conclude the existence of (maximal) canard solutions along which the attracting and the repelling slow manifold intersect.

Note that one canard solution is passing from the repelling to the attracting slow manifold. Canard solutions with such a behaviour are called *faux canards*.
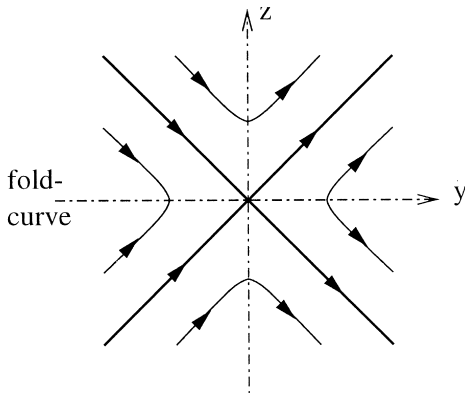
**FIG. 1.** Reduced flow and singular canards (straight lines) projected to the $(y, z)$-plane.

Similar explicit solutions of leading order approximations will play a crucial role in our analysis of canards.

In Section 2 we define and classify canard points in $\mathbb{R}^3$ (on the fold-curve of a two-dimensional folded critical manifold) depending on the dynamics of the reduced flow near the fold-curve. At a canard point there is a possibility for the reduced flow to cross the fold-curve in finite time, similar to the above example. In correspondence with the phase portrait of the (desingularized) reduced flow at these points, we classify the canard points as *folded saddles, folded nodes*, and *folded saddle-nodes*. The canard point in the above mentioned example is a folded saddle. The aim of this work is to prove the existence of canards near solutions of the reduced flow passing through these canard points.

The pioneering work on canards in $\mathbb{R}^3$ is due to Benoit [Ben83, Ben90]. Based on methods from nonstandard analysis he analysed the existence of canard solutions in the folded saddle and in the folded node case. Similar results by means of matched asymptotic expansion can be found in [MKKR94]. In [MS01] a model of a chemical oscillator involving a folded saddle-node is analysed by using the geometric theory and blow-up. We refer to the problem considered in [MS98] also as a prototypical example of complicated global bifurcations (known as *mixed-mode-oscillations*) involving canards in three-dimensions.

In Section 3 we describe *blow-up* of singularities in a form suitable for the application to geometric singular perturbation analysis. Our exposition follows closely [Rou93], see also [Dum93, DR96]. For a detailed expository presentation of the blow-up method in the context of singular perturbation problems we refer to [KS01b]. A blow-up is essentially a clever

coordinate transformation by which a degenerate point is "blown-up" to a sphere (in more complicated problems other manifolds arise). In certain directions transverse to the sphere and even on the sphere one gains enough hyperbolicity to allow a complete analysis. The technique is a generalization of the well known blow-up method for degenerate equilibria of planar vector fields. To apply this idea to singular perturbation problems the singular perturbation parameter $\varepsilon$ must be included in the blow-up! By construction the blown-up locus (the sphere) is invariant. Surprisingly often the equations governing the dynamics on the sphere are integrable in some sense or at least some special solutions can be found. We remark that the latter situation will be relevant in the present analysis. By blowing up the "fine structure" of the singular perturbation problem becomes visible and the full problem can be analysed by applying or adapting standard methods from dynamical systems theory.

Using this technique we prove in Section 4 the existence of canards in the case of a folded saddle. Furthermore we show that canards exist for the folded node case provided a (generic) non-resonance condition is satisfied. Geometrically the resonances are related to the twisting of the attracting and repelling slow manifold around the canard solution. At a resonance a bifurcation of canards may occur because the intersection of the repelling and the attracting slow manifold is non-transverse.

## 2. DYNAMICS OF THE REDUCED PROBLEM AND CLASSIFICATION OF CANARDS

We assume that the critical manifold $S = \{(x, y, z) : f(x, y, z, 0) = 0\}$ of system (1) is a nondegenerate folded surface in a neighbourhood of the origin. Sufficient conditions for this assumption are

$$(6) \qquad \begin{aligned} f(0, 0, 0, 0) &= 0, & f_z(0, 0, 0, 0) &= 0, \\ f_x(0, 0, 0, 0) &\neq 0, & f_{zz}(0, 0, 0, 0) &\neq 0. \end{aligned}$$

Under these conditions the origin is a non-hyperbolic equilibrium of the layer problem. Under the above assumptions the fold-curve can be parameterized by $y$, i.e., points on the fold-curve are given by $(\xi(y), y, \zeta(y))$, $y \in I$. Following [MKKR94], we define

$$l(y) := \begin{pmatrix} f_x \\ f_y \end{pmatrix} \cdot \begin{pmatrix} g_1 \\ g_2 \end{pmatrix} \bigg|_{(\xi(y), y, \zeta(y), 0)}.$$

The nature of the reduced flow of system (1) depends crucially on whether the *transversality condition* $l(0) \neq 0$ is satisfied or not. The geometric meaning

of the transversality condition, which is called the normal switching condition in [MKKR94], is that the projection of the reduced flow into the $(x, y)$-plane is not tangent to the fold-curve at the origin.

The regular fold case corresponds to situations where the transversality condition is satisfied. In this case the reduced flow is directed towards (or away from) the fold-curve on both branches of the critical manifold. Thus, the only possibility for solutions reaching the fold-curve is to jump. This behaviour is quite similar to the regular fold case in planar systems. If the transversality condition is satisfied it holds for a segment of the fold-curve; i.e., there exists always a segment of jump points. We refer to [Wec98, SW99] for a geometric analysis of this case. In this work we consider the case where the transversality condition is violated, i.e.,

$$(7) \qquad\qquad\qquad l(0) = 0.$$

As will become clear later, the condition $l(0) = 0$ is necessary for the existence of canards in system (1).

PROPOSITION 2.1. *Assume that system* (1) *satisfies conditions* (6) *and* (7). *Then there exists a smooth change of coordinates which brings system* (1) *to the form*

$$
\begin{aligned}
(8) \qquad & \dot{x} = by + cz + O(x, \varepsilon, y^2, yz, z^2) \\
& \dot{y} = a + O(x, y, z, \varepsilon) \\
& \varepsilon\dot{z} = x + z^2 + O(\varepsilon x, \varepsilon y, \varepsilon z, \varepsilon^2, x^2 z, z^3, xyz),
\end{aligned}
$$

*in a neighborhood of the origin, with computable constants* $(a, b, c) \in \mathbb{R}^3$. *If* $l'(0) \neq 0$ *holds then* $b \neq 0$. *If* $g_2(0, 0, 0, 0) \neq 0$ *holds then* $a \neq 0$.

*Proof.* The implicit function theorem gives a parameterization $(\xi(y), y, \zeta(y))$, $y \in I$, of the fold-curve for a suitable interval $I$. In a first step a coordinate transformation $(x, y, z) \mapsto (x - \xi(y), y, z - \zeta(y))$ in system (1) rectifies the fold-curve along the $y$-axis. Taylor expansion of the functions $f, g_1, g_2$ together with a sequence of linear and near identity transformations gives the result. ∎

Setting $\varepsilon = 0$ in system (8) yields the reduced problem

$$
\begin{aligned}
(9) \qquad & \dot{x} = by + cz + O(x, y^2, yz, z^2) \\
& \dot{y} = a + O(x, y, z) \\
(10) \qquad & 0 = x + z^2 + O(x^2, z, z^3, xyz).
\end{aligned}
$$

The reduced problem is a two-dimensional dynamical system on the critical manifold $S$ defined by the algebraic equation (10). The implicit function theorem implies that the folded critical manifold is a graph $S = \{(x(y, z), y, z)\}$ in a neighbourhood of the origin with

$$x(y, z) = -z^2(1 + O(y, z)),$$

i.e., the manifold $S$ is approximately a parabolic cylinder near the origin. Let $S_a$ resp. $S_r$ denote the lower resp. upper branch and let $F$ denote the fold-curve, so that $S = S_a \cup F \cup S_r$. The transformed system (8) satisfies $f_{zz}(0, 0, 0, 0) > 0$ which implies that the branch $S_a$ is attracting while $S_r$ is repelling for the corresponding layer problem, which explains the notation. Points on the fold-curve $F$ are non-hyperbolic, weakly attracting from below and weakly repelling upwards (see Fig. 2).

We differentiate the function $x(y, z)$ with respect to time and substitute for $\dot{x}$ in (9) to obtain

(11)
$$\dot{y} = a + O(y, z)$$
$$-2z(1 + O(y, z)) \dot{z} = by + cz + O(y^2, yz, z^2).$$

System (11) is the projection of the reduced vector field into the $(y, z)$-plane near the origin. System (11) is singular at the fold-curve, i.e., at $z = 0$. The standard existence and uniqueness results for differential equations do not hold there. In particular different solutions of system (11) may approach the same point on the fold-curve in finite forward or backward
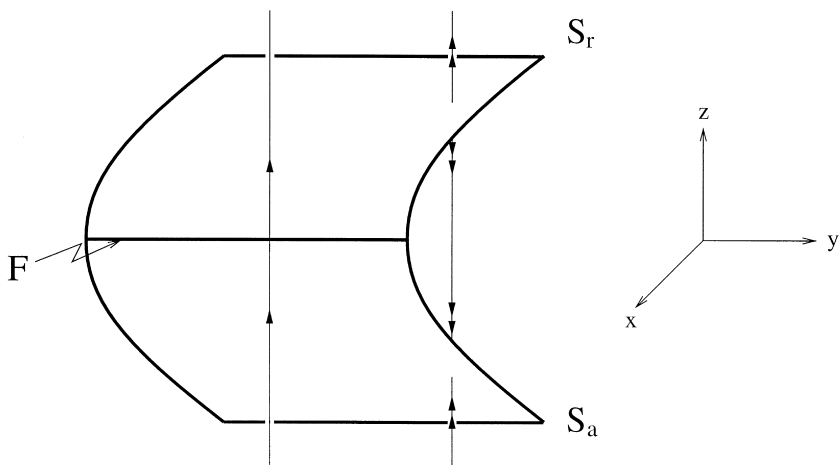


**FIG. 2.**  Critical manifold, attracting and repelling branch.

time. We will see that this allows the existence of solutions of the reduced problem which pass from $S_a$ to $S_r$ through the origin or vice versa.

To obtain the dynamics of system (11) we multiply the right hand by $-2z(1 + O(y, z))$ and divide the second equation by this factor to obtain the *desingularized system*

$$
\begin{aligned}
(12) \qquad \dot{y} &= -2az + O(yz, z^2) \\
\dot{z} &= by + cz + O(y^2, yz, z^2).
\end{aligned}
$$

We study the phase portrait of system (12) in a neighbourhood of the origin. It has the same phase portrait as system (11) on $S_a$, i.e., for $z < 0$. On $S_r$, that is for $z > 0$, time has to be reversed in the phase portrait of (12) to obtain the phase portrait of the reduced system (11).

The origin is an equilibrium of the desingularized system (12). In the following we discuss the type of the equilibrium at the origin depending on the parameters $(a, b, c)$.

The eigenvalues of the linearization of system (12) at the origin are $\lambda_{1,2} = (c \pm \sqrt{c^2 - 8ab})/2$.

LEMMA 2.1.   *For $c < 0$ the origin is an equilibrium of the desingularized system* (12) *of the following type:*

$$
\begin{aligned}
(13) \qquad & ab < 0, & \lambda_1 < 0 < \lambda_2 & & \textit{saddle,} \\
& ab = 0, & \lambda_1 < 0 = \lambda_2 & & \textit{saddle-node,} \\
& 0 < 8ab < c^2, & \lambda_1 < \lambda_2 < 0 & & \textit{node,} \\
& 8ab = c^2, & \lambda_1 = \lambda_2 < 0 & & \textit{degenerate node,} \\
& c^2 < 8ab, & Re(\lambda_i) < 0 & & \textit{focus.}
\end{aligned}
$$

*Remark.*   These results also hold for $c > 0$, just the eigenvalues change their signs. The case $c = 0$ is discussed later.

The eigenvectors are given by $v_{1,2} = (1, -\lambda_{1,2}/2a)$ for $a \neq 0$ and by $v_1 = (0, 1)$, $v_2 = (1, -b/c)$ for $a = 0$. In the following we use the terminology saddle, saddle-node, node and focus case corresponding to the type of the equilibrium of the desingularized system. For $8ab = c^2$ there exists just one eigenvector (double eigenvalue $c/2$). Hence, we call this case the degenerate node.

In the case $ab = 0$ we are in a saddle-node situation due to the zero eigenvalue of the equilibrium of the desingularized system for $c \neq 0$. We distinguish two subcases $(a \neq 0, b = 0)$ resp. $(a = 0, b \neq 0)$. The more degenerate case $(a = 0, b = 0)$ is not considered in the following.

In the case $(a \neq 0, b = 0)$ the eigenvectors are given by $v_1 = (1, -c/2a)$, $v_2 = (1, 0)$; i.e., the center-flow corresponding to the zero eigenvalue is tangent to the fold-curve at the origin. In this case the phase portrait near the equilibrium depends on the higher order terms.

In the case $(a = 0, b \neq 0)$ the eigenvectors are given by $v_1 = (0, 1)$, $v_2 = (1, -b/c)$; i.e., the eigenvector corresponding to the nonzero eigenvalue is orthogonal to the fold-curve at the origin and the center manifold is transverse to the fold-curve. The flow on the center manifold depends on higher order terms.

The phase portraits of the reduced system (11) in all cases described in Lemma 2.1 are obtained by changing the direction of the flow in the phase portraits of the desingularized system (12) for positive $z$. Considered as a singular point of the reduced flow we call the origin a *folded saddle, folded saddle-node, folded node, folded degenerate node*, or *folded focus*. All cases are shown in Fig. 3. The figures for the folded saddle-node case show the least degenerate phase portraits compatible with our assumptions.

Note that the singularity at the origin is not an equilibrium for the reduced system (11). Solutions of the desingularized system (12) which approach the origin in backward or forward time in a hyperbolic direction correspond to solutions of the reduced problem (11) passing through the origin with nonzero speed. This is due to a cancellation of a simple zero in the second equation in system (11). However, in center directions solutions of the reduced problem approach the origin asymptotically in backward or forward time. More specifically we consider the following distinguished solutions of the reduced problem:

In the case of the folded saddle there exist two solutions passing through the origin, i.e. a solution $\Gamma_1$ corresponding to the stable manifold of the saddle and a solution $\Gamma_2$ corresponding to the unstable manifold of the saddle of the desingularized system.

In the folded node case there exists a unique solution $\Gamma_1$ corresponding to the strong stable manifold of the origin. All other solutions passing through the origin are tangent to the weak eigendirection at the origin.

In the degenerate node case all solutions passing through the origin are tangent to the (unique) eigenvector.

In the folded saddle-node case a unique solution $\Gamma_1$ corresponding to the strong stable manifold of the saddle-node of the desingularized system passes through the origin.

The unique solutions are shown as bold lines in the phase portraits of Fig. 3. The dashed lines correspond to the tangent direction of the non-unique solutions passing through the origin.

The classification scheme (13) holds for $c \neq 0$. For $c = 0$ the relevant eigenvalues are $\lambda_{1,2} = \mp \sqrt{-2ab}$ and we obtain:
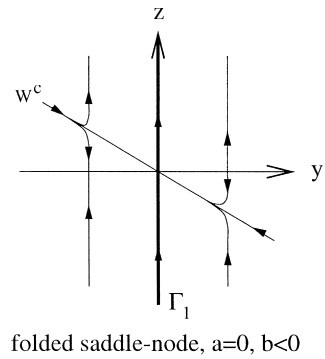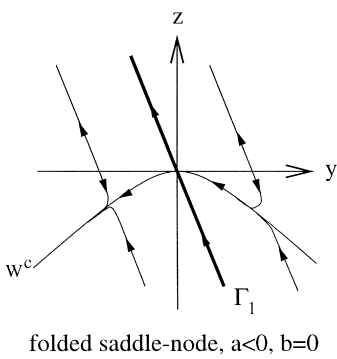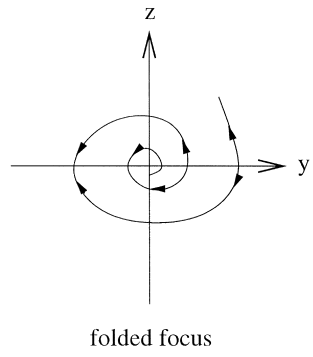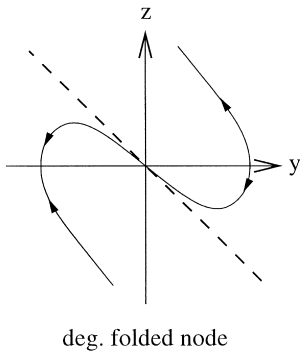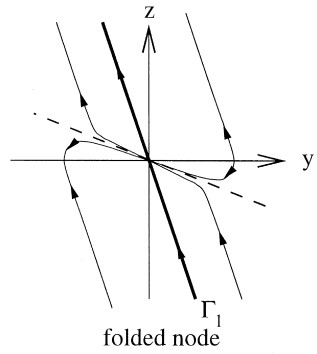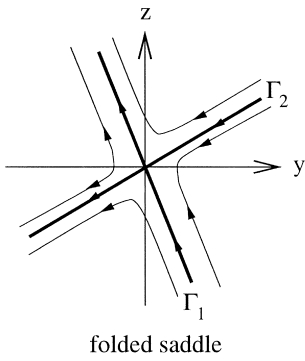
FIG. 3.  Phase portrait of reduced flow, $c < 0$, $a \leqslant 0$.

LEMMA 2.2. *For $c = 0$ the equilibrium at the origin of the desingularized system* (12) *is of the following type:*

$$
\begin{array}{lll}
(14) & \begin{array}{l} ab < 0, \\ ab = 0, \\ ab > 0, \end{array} & \begin{array}{l} \lambda_1 < 0 < \lambda_2 \\ \lambda_{1,2} = 0 \\ Re(\lambda_{1,2}) = 0 \end{array} & \begin{array}{l} saddle, \\ nilpotent, \\ center. \end{array}
\end{array}
$$

The saddle case is analogous to the saddle case in (13). The other two degenerate cases are not considered in this work. Note that in the introductory example (5) the origin is a folded saddle with $c = 0$. Figure 4 shows the bifurcation diagram for the equilibrium of the desingularized system (12).

DEFINITION 2.1. Solutions of the reduced problem passing through a canard point from an attracting critical manifold to a repelling critical manifold are called *singular canards*.

Solutions of the reduced problem passing through a canard point from a repelling critical manifold to an attracting critical manifold are called *singular faux canards*.

The following observation follows immediately from the classification (13) and the phase portraits in Fig. 3.
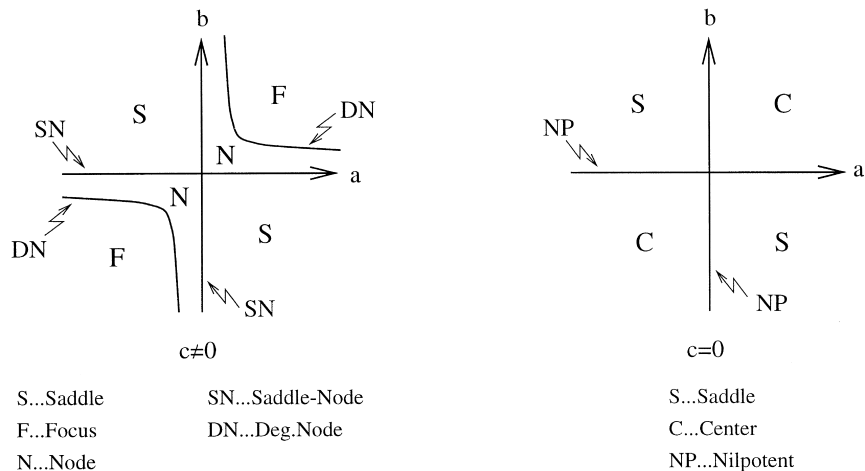


S...Saddle          SN...Saddle-Node          S...Saddle
F...Focus           DN...Deg.Node             C...Center
N...Node                                       NP...Nilpotent

**FIG. 4.** Bifurcation diagram, $c \neq 0$ and $c = 0$.

LEMMA 2.3.  *A singular canard corresponds to a negative eigenvalue* $\lambda_i$, $i = 1, 2$. *A singular faux canard corresponds to a positive eigenvalue.*

*Remark.*  In the folded saddle case there exists always one singular canard and one singular faux canard. In all other cases there exist either just singular canards or just singular faux canards.

The following example shows the occurrence of canard points in a specific problem.

EXAMPLE 2.1.  Consider the forced van der Pol oscillator

(15)
$$\dot{x} = -z + A \cos \varphi$$
$$\dot{\varphi} = \omega$$
$$\varepsilon \dot{z} = x - \tfrac{1}{3} z^3 + z,$$

with parameters $A, \omega > 0$ and $(x, \varphi, z) \in \mathbb{R} \times S^1 \times \mathbb{R}$. We will show that all singularities of the above classification scheme are realized as $A$ varies. The critical manifold is an S-shaped surface given as a graph $x(z, \varphi) = \frac{1}{3} z^3 - z$ containing two fold-curves for $z = \pm 1$. The reduced flow on the critical manifold is given by

(16)
$$(z^2 - 1)\, \dot{z} = -z + A \cos \varphi$$
$$\dot{\varphi} = \omega.$$

At the fold-curves $z = \pm 1$ the reduced flow is singular. The corresponding desingularized system is

(17)
$$\dot{z} = -z + A \cos \varphi$$
$$\dot{\varphi} = \omega(z^2 - 1).$$

The phase portrait of the reduced system is obtained by changing the direction of the flow in the phase portrait of system (17) for $|z| < 1$. We discuss the bifurcations of the reduced flow as the amplitude of the forcing $A$ varies.

For $A < 1$ system (17) has no equilibrium, just an unstable cycle on the repelling critical manifold. All points on the fold-curves $z = \pm 1$ are jump points (see Fig. 5).

As the amplitude of the forcing increases to the value $A = 1$ two singular points $(z = 1, \varphi = 0)$ and $(z = -1, \varphi = \pi)$ of system (17) are created which

A<1

**FIG. 5.** Reduced flow of forced van der Pol oscillator, unstable cycle, and jump points.

split up in two pairs of singular points at $(z = 1, \varphi = \mp \arccos(1/A))$ and $(z = -1, \varphi = \pi \mp \arccos(1/A))$ for $A > 1$. This creation of critical points for the desingularized system by variation of the parameter $A$ is a standard saddle-node bifurcation. Hence, for $A = 1$ the singular points are folded saddle-nodes and for $A > 1$ a folded saddle and a folded node exist on each fold-curve (see Fig. 6). In the following figures only the dynamics close to the canard points on the fold-curve $z = 1$ is shown.

A simple eigenvalue calculation shows that the folded saddles exist for all $A > 1$. The folded nodes are restricted to the interval $1 < A < \bar{A}$ with $\bar{A} = \sqrt{1 + 1/64\omega^2}$. For $A = \bar{A}$ the folded nodes are degenerate folded nodes and for $A > \bar{A}$ they become folded foci (see Fig. 7).



**FIG. 6.** Reduced flow of forced van der Pol oscillator, $A = 1$, folded saddle-node; $1 < A < \bar{A}$, folded saddle and folded node.
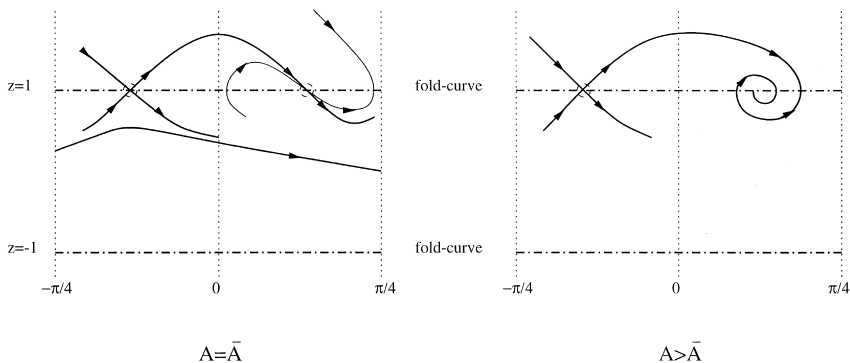
**FIG. 7.** Reduced flow of forced van der Pol oscillator, $A = \bar{A}$, folded saddle and deg. folded node; $A > \bar{A}$, folded saddle and folded focus.

*Remark.* Numerical simulation shows that the unstable cycle exists for $A < \tilde{A}$, with $\tilde{A} > \bar{A}$. At $A = \tilde{A}$ the unstable cycle ends in a heteroclinic cycle connecting the folded saddles. The heteroclinic cycle breaks for $A > \tilde{A}$.

We are interested in the persistence of singular canards under small perturbations; i.e., we are interested in the existence of maximal canards nearby.

As a starting point for our analysis we briefly review some properties of the slow manifolds $S_{a,\varepsilon}$ resp. $S_{r,\varepsilon}$. For the layer problem the critical manifold $S$ is a manifold of equilibria. At each point of $S_a$ there exist stable fibers of the layer flow. These fibers form a foliation of $W^s(S_a)$ in an open neighbourhood of $S_a$. Similarly, a foliation of $W^u(S_r)$ exists in an open neighbourhood of $S_r$ (see Fig. 2). If follows from the standard theory [Fen79] that outside a small neighbourhood $U$ of the fold-curve the manifolds $S_a$ and $S_r$ perturb smoothly to locally invariant manifolds $S_{a,\varepsilon}$ and $S_{r,\varepsilon}$ for sufficiently small $\varepsilon \neq 0$. Moreover, there exist smooth invariant foliations of the manifold $W^s(S_{a,\varepsilon}) \cap V_1$ in a neighbourhood $V_1$ of the base $S_{a,\varepsilon}$ and smooth invariant foliations of the manifold $W^u(S_{r,\varepsilon}) \cap V_2$ in a neighbourhood $V_2$ of the base $S_{r,\varepsilon}$.

Recall that the slow manifolds are obtained as sections $\varepsilon = const.$ of three-dimensional, locally invariant, center-like manifolds $M_a$ resp. $M_r$ of the extended system

$$
\begin{aligned}
x' &= \varepsilon(by + cz + O(x, \varepsilon, y^2, yz, z^2)) \\
y' &= \varepsilon(a + O(x, y, z, \varepsilon)) \\
z' &= x + z^2 + O(\varepsilon x, \varepsilon y, \varepsilon z, \varepsilon^2, x^2 z, z^3, xyz) \\
\varepsilon' &= 0
\end{aligned}
\tag{18}
$$

in the extended phase space $\mathbb{R}^4$. For the extended system $S \times \{0\}$ is a manifold of equilibria. Outside of a neighbourhood $U$ of the fold-curve the linearization of (18) at points $S_a \times \{0\}$ has a triple zero eigenvalue and one negative eigenvalue uniformly bounded away from zero. This allows to prove the existence of the attracting center-like manifold $M_a$. The repelling center-like manifold $M_r$ is obtained in a similar way. At the fold-curve the linearization has a quadruple zero eigenvalue and the construction of the slow manifolds breaks down. Clearly, the slow manifolds can be extended in forward and backward time by the flow, however, their behaviour is then not controlled by the singular limit problems introduced so far.

In the next section we describe the blow-up technique which allows to analyse system (18) near the fold-curve.

## 3. BLOW-UP

We have seen that points on the fold-curve are more degenerate equilibria of system (18) than the other points of the critical manifold $S$. The linearization of system (18) has a quadruple zero eigenvalue along the fold-curve while the linearization at the other points of the critical manifold $S$ has a triple zero eigenvalue and one negative resp. positive eigenvalue for $z < 0$ resp. $z > 0$.

The important insight in [DR96] is that the blow-up technique is the right tool to desingularize nilpotent equilibria like the points on the fold-curve, viewed as degenerate equilibria of the extended system (18). The blow-up technique is essentially a clever coordinate transformation by which a degenerate equilibrium is blown-up to an $m$-sphere with appropriate $m$. With this procedure one gains enough hyperbolicity to allow for a complete analysis by standard techniques. For nilpotent equilibria of planar vector fields the blow-up technique is well known, see, e.g., [GH83, Dum91]. In the sequel we will give a sketch of the blow up-technique in the context needed for the analysis of the extended system (18). For a description of the general technique and background material we refer to [DR91, Rou93]. Our exposition in the context of singular perturbation follows closely [KS01b]. We consider an extended system in $\mathbb{R}^4$

$$
\begin{aligned}
x' &= \varepsilon g_1(x, y, z, \varepsilon) \\
y' &= \varepsilon g_2(x, y, z, \varepsilon) \\
z' &= f(x, y, z, \varepsilon) \\
\varepsilon' &= 0.
\end{aligned}
$$
(19)

Let $X$ denote the vector field corresponding to (19). Assume $X(0) = 0$ and $f_z(0, 0, 0, 0) = 0$, i.e. the origin is a nilpotent equilibrium. The blow-up transformation is defined as a mapping

$$\Phi : B_0 \subset B \to \mathbb{R}^4$$
$$(\bar{x}, \bar{y}, \bar{z}, \bar{\varepsilon}, \bar{r}) \mapsto (\bar{r}^{\delta_1}\bar{x}, \bar{r}^{\delta_2}y, \bar{r}^{\delta_3}\bar{z}, \bar{r}^{\delta_4}\bar{\varepsilon})$$

with the manifolds $B = \mathbb{S}^3 \times \mathbb{R}$, $B_0 = \mathbb{S}^3 \times [-r_0, r_0]$, $r_0 > 0$ and the weights $(\delta_1, \delta_2, \delta_3, \delta_4) \in \mathbb{Z}^4$; i.e., the origin is blown-up by $\Phi$ to a three-sphere with $\bar{x}^2 + \bar{y}^2 + \bar{z}^2 + \bar{\varepsilon}^2 = 1$.

The map $\Phi$ is surjective and proper, because it maps the 3-sphere $Z = \mathbb{S}^3 \times \{0\}$ to the origin, i.e., $\Phi^{-1}(0) = Z$. Furthermore $\Phi|_{B \setminus Z}$ is a diffeomorphism from $B \setminus Z$ to $\mathbb{R}^4 \setminus \{0\}$. The map $\Phi$ defines the induced map $\Phi_* : TB \to T\mathbb{R}^4$ between the associated tangent bundles.

Since $X(0) = 0$ the map $\Phi$ induces a vector field $\bar{X}$ on $B$ such that $\Phi_* \bar{X} = X$ (see Fig. 8). It suffices to study $\bar{X}$ on $B_0$ since $\Phi(B_0)$ is a full neighbourhood of the origin. For the analysis of $\bar{X}$ on $B_0$ we have to introduce charts for the manifold $B$. Charts are homeomorphic maps $\kappa_i : B_i \to \mathbb{R}^4$ with $i \in I$ and $B = \bigcup_{i \in I} B_i$. Again, the map $\Phi$ induces vector fields $X_i$ on $B_i$ for all $i \in I$.

To make calculations in the charts $\kappa_i$ as simple as possible, we will use directional blow-ups $\Phi_i$ which lead to directional charts $\kappa_i$.

DEFINITION 3.1. Directional blow-ups $\Phi_i$, $i = 1, ..., 2m$ are obtained by setting one blown-up variable on $\mathbb{S}^m$ equal to $\pm 1$ in the definition of the mapping $\Phi$. The directional charts $\kappa_i$, $i = 1, ..., 2m$ are defined such that the diagram in Fig. 9 commutes. In chart $\kappa_i$ the blown-up vector field $\bar{X}$ is described by a vector field $X_i$, $i = 1, ..., 2m$.

$$
\begin{array}{ccc}
TB & \xrightarrow{\;\Phi_*\;} & T\mathbb{R}^4 \\[2mm]
\bar{X} \uparrow & & \uparrow X \\[2mm]
B & \xrightarrow[\;\Phi\;]{} & \mathbb{R}^4
\end{array}
$$

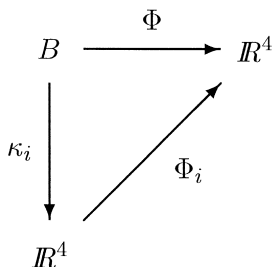**FIG. 8.** Commutative diagram for the induced vector field.

**FIG. 9.** Commutative diagram for the directional charts $\kappa_i$.

The charts $\kappa_i$, $i = 1, \ldots, 2m$ cover the $m$-sphere by $m$-planes perpendicular to the axes. In our applications only some of these charts are needed. In the following the subscripts for the individual charts are chosen according to the order in which the charts are used in the analysis.

In singular perturbation problems the chart $\kappa_2$ corresponding to $\bar{\varepsilon} = 1$ in the mapping $\Phi$ is the most important chart. The corresponding directional blow-up is

$$\Phi_2 \colon \mathbb{R}^4 \to \mathbb{R}^4$$
$$(x_2, y_2, z_2, r_2) \mapsto (r_2^{\delta_1} x_2, r_2^{\delta_2} y_2, r_2^{\delta_3} z_2, r_2^{\delta_4}).$$

This transformation is an $\varepsilon$-dependent rescaling of the variables $(x, y, z)$ since $r_2 = \varepsilon^{-\delta_4}$; i.e., the vector field $X_2$ is obtained by rescaling the original variables. To emphasize the importance of the chart $\kappa_2$ we call this chart the *classical chart*. In this chart $r_2$ acts just as a parameter due to the equation $\varepsilon' = 0$ which implies $r_2' = 0$ for the vector field $X_2$.

In $\kappa_2$ the plane $r_2 = 0$ is the blown-up image of the singular point at the origin. Hence, the vector field $X_2$ vanishes on the plane $r_2 = 0$.

In the following we introduce the notion of a local vector field and the operation of local division for local vector fields which are needed to desingularize the blown-up vector field.

DEFINITION 3.2. A local vector field $X$ is defined on a compact smooth manifold $B$ by a finite open covering $\{B_i\}$ of $B$ with some smooth vector field $X_i$ on each $B_i$, such that for each pair of indices $i, j \in I$ with $B_i \cap B_j \neq \varnothing$ there exists a smooth function $g_{ij}$ defined and strictly positive in $B_i \cap B_j$ such that $X_i = g_{ij} X_j$ on $B_i \cap B_j$.

*Remark.* A local vector field defines a phase portrait just as a vector field. However, one allows different time parameterization of orbits in each $B_i$, $i \in I$.

DEFINITION 3.3.   Let $\{B_i\}$ be a finite open covering of $B$, on which local vector fields $X$ and $\tilde{X}$ are given by $X_i$ and $\tilde{X}_i$. $\tilde{X}$ is the result of local division of $X$ if there exists smooth functions $f_i: B_i \to \mathbb{R}$ such that $X_i = f_i \tilde{X}_i$ in $B_i$.

*Remark.*   In general these functions $f_i$ are arbitrary. In our application the functions $f_i$ vanish only on $Z$, i.e., where the blow-up transformation fails to be a diffeomorphism. In more practical terms our application of local division consists of dividing out powers of $r_i$ and this leads to vector fields $\tilde{X}_i$ and $X_i$ with the same phase portrait for $r_i > 0$. However, on the set $r_i = 0$ the vector field $\tilde{X}_i$ may show nontrivial dynamics which has been invisible for $X_i$.

For each specific problem suitable weights $(\delta_1, \delta_2, \delta_3, \delta_4)$ have to be chosen. The choice of the weights is guided by the following requirements:

1.   local division is possible to obtain the vector fields $\tilde{X}_i$;

2.   the vector fields $\tilde{X}_i$ have only hyperbolic or semi-hyperbolic equilibria;

3.   the dynamics in the planes $r_i = 0$ can be analysed;

4.   perturbation methods can be used to obtain the dynamics for $r_i > 0$.

We will see that the proper weights are most effectively determined in the classical chart. With the proper choice the truncation of the vector field $\tilde{X}_2$ obtained by setting $r_2 = 0$ can be viewed as a normal form of the original problem; i.e., it is the simplest possible description of the underlying phenomena. In the applications which we have in mind it is always necessary to consider the dynamics of this normal form (in the classical chart) on unbounded domains. Otherwise a simple rescaling would suffice, which means that the problem is not singularly perturbed. Points at infinity in the classical chart correspond to points on the "equator" on the sphere in the blow-up. To capture the dynamics near the "equator" we need additional charts $\kappa_i$, $i \neq 2$. In these other charts the variables $r_i$ become dynamic variables.

We summarize the above description of the blow-up technique in the form appropriate for the extended system (19) in:

DEFINITION 3.4.   A desingularization of a vector field $X$ in $\mathbb{R}^4$ with a nilpotent equilibrium $X(0) = 0$ is a blow-up transformation $\Phi: B \to \mathbb{R}^4$ with $Z = \Phi^{-1}(0)$ a 3-sphere and suitable weights $(\delta_1, \delta_2, \delta_3, \delta_4)$ such that for all local vector fields $X_i$ induced by $\Phi$ and for any point $p \in Z_i = \Phi_i^{-1}(0)$ with $\tilde{X}_i(p) = 0$, where $\tilde{X}_i$ is a result of local division by $X_i$, the point $p$ is a hyperbolic or semihyperbolic singularity of the vector field $\tilde{X}_i$.

It is possible that after one blow-up some nilpotent equilibria remain. Then additional blow-ups can be used to desingularize these nilpotent equilibria. Thus, the blow-up technique can be seen as an iterative procedure.

We will need to change coordinates between the charts to connect the dynamics in the different charts.

DEFINITION 3.5. The change of coordinates between two charts $\kappa_i$ and $\kappa_j$ is defined as

$$\kappa_{ji} := \kappa_j \circ \kappa_i^{-1}.$$

We introduce the following notation: $\bar{P}$ denotes an object in the blow-up which corresponds to an object $P$ in the original problem. If $\bar{P}$ is described in a chart $\kappa_i$ then $P_i$ denotes the object in this chart.

The most subtle part of the blow-up technique is to find the weights $(\delta_1, \delta_2, \delta_3, \delta_4)$ suitable for the desingularization. In singular perturbation problems the weights are closely related to the rescalings used in the method of matched asymptotic expansions. In fact a problem corresponding to the blown-up vector field written in the classical chart lies at the core of many of the existing classical treatments of such problems. Thus, the weights for many singular perturbation problems are already known in the literature.

The weights suitable for system (18) are $(\delta_1, \delta_2, \delta_3, \delta_4) = (2, 1, 1, 2)$, which can be found in [Ben83] resp. in [Bra93] for a certain subcase. A theory for obtaining the weights is often associated with the notion of *Newton Polyhedra* of polynomial vector fields. For a detailed description of the existing theory we refer to [Bru80, BM90]. However, the theory of Newton Polyhedra is less useful for higher dimensional problems since a general method to determine the weights needed in a blow-up seems not to exist.

In the next section we apply the blow-up method to analyse the behaviour and possible intersections of the extended manifolds $M_a$ resp. $M_r$ of system (18).

## 4. ANALYSIS OF CANARDS

Recall the extended system (18) and that the slow manifolds $S_{a,\varepsilon}$ and $S_{r,\varepsilon}$ are obtained as sections $\varepsilon = const.$ of three-dimensional center-like manifolds $M_a$ resp. $M_r$. All calculations are done in the extended phase space, but some of our results are stated in sections $\varepsilon = const.$ of the extended

phase space. Outside of an arbitrary small neighbourhood $U$ of the fold-curve the manifolds $S_a$ and $S_r$ perturb smoothly to locally invariant manifolds $S_{a,\varepsilon}$ and $S_{r,\varepsilon}$ for sufficiently small $\varepsilon \neq 0$. The goal is to investigate whether the extensions of the slow manifold $S_{a,\varepsilon}$ resp. $S_{r,\varepsilon}$ in forward resp. backward time by the flow do intersect.

The possible reduced flows of system (18) are described in (13) and are shown in Fig. 3. In all cases except the focus case singular canards exist; i.e., there exist solutions in the reduced problem which pass at the origin from the attracting to the repelling branch of the critical manifold or vice versa. The following theorem is the main result of this work:

THEOREM 4.1. *Assume system* (8). *In the folded saddle and in the folded node case singular canards $\Gamma_1$ perturb to maximal canard solutions for sufficiently small $\varepsilon$.*

*For a folded node with $\lambda_1 < \lambda_2 < 0$ a maximal canard solution corresponding to the weak eigendirection exists for sufficiently small $\varepsilon$ provided that*

$$\mu_2 := \frac{\lambda_1}{\lambda_2}$$

*is* **not** *a natural number*.

The main idea of the proof is as follows. We use the blow-up transformation $\Phi: B = \mathbb{S}^3 \times \mathbb{R} \to \mathbb{R}^4$ given by

$$(20) \qquad x = r^2\bar{x}, \qquad y = r\bar{y}, \qquad z = r\bar{z}, \qquad \varepsilon = r^2\bar{\varepsilon},$$

with $(\bar{x}, \bar{y}, \bar{z}, \bar{\varepsilon}) \in \mathbb{S}^3$. It turns out that it suffices to consider two charts $\kappa_1$ and $\kappa_2$ defined by $\bar{x} = -1$ resp. $\bar{\varepsilon} = 1$. For the blown-up vector field we obtain special solutions (in the classical chart $\kappa_2$) which can be viewed as extensions of the singular canards. The additional chart $\kappa_1$ is used to connect the unbounded branches (in forward and backward time) of the special solutions with the singular canards of the reduced problem. We will show that under the conditions of Theorem 4.1 the extensions of the slow manifolds along these special solutions in chart $\kappa_2$ intersect transversally which proves the existence of maximal canard solutions in the extended system (18).

LEMMA 4.1. *The change of coordinates between chart $\kappa_1$ and chart $\kappa_2$ is given by*

$$(21) \qquad \kappa_{12}(x_2, y_2, z_2, r_2) = \left( r_2\sqrt{-x_2}, \frac{y_2}{\sqrt{-x_2}}, \frac{z_2}{\sqrt{-x_2}}, \frac{1}{-x_2} \right), \qquad x_2 < 0,$$

$$(22) \qquad \kappa_{21}(r_1, y_1, z_1, \varepsilon_1) = \left( \frac{-1}{\varepsilon_1}, \frac{y_1}{\sqrt{\varepsilon_1}}, \frac{z_1}{\sqrt{\varepsilon_1}}, r_1\sqrt{\varepsilon_1} \right), \qquad \varepsilon_1 > 0.$$

4.1. *Dynamics in the Classical Chart $\kappa_2$*

We consider transformation (20) with $\bar{\varepsilon} = 1$; i.e., we consider the directional blow-up $\Phi_2 : \mathbb{R}^4 \to \mathbb{R}^4$ given by

$$\Phi_2(x_2, y_2, z_2, r_2) = (r_2^2 x_2, r_2 y_2, r_2 z_2, r_2^2).$$

This transformation is just an $\varepsilon$-dependent rescaling of $(x, y, z)$, since $r_2 = \sqrt{\varepsilon}$. After transformation of system (18) and desingularization of the blown-up vector field we obtain

$$
\begin{aligned}
(23) \qquad & x_2' = b y_2 + c z_2 + r_2 h_1(x_2, y_2, z_2, r_2) \\
& y_2' = a + r_2 h_2(x_2, y_2, z_2, r_2) \\
& z_2' = x_2 + z_2^2 + r_2 h_3(x_2, y_2, z_2, r_2) \\
& r_2' = 0,
\end{aligned}
$$

with

$$
\begin{aligned}
h_1(x_2, y_2, z_2, r_2) &= \beta_1 x_2 + \beta_2 + \beta_3 y_2^2 + \beta_4 z_2^2 + \beta_5 y_2 z_2 + O(r_2) \\
h_2(x_2, y_2, z_2, r_2) &= \gamma_1 y_2 + \gamma_2 z_2 + O(r_2) \\
h_3(x_2, y_2, z_2, r_2) &= \alpha_1 z_2^3 + \alpha_2 y_2 + \alpha_3 z_2 + O(r_2).
\end{aligned}
$$

Since $r_2' = 0$, this blown-up system is still a family of vector fields with parameter $r_2$. Setting $r_2 = 0$ gives the unperturbed problem

$$
\begin{aligned}
(24) \qquad & x_2' = b y_2 + c z_2 \\
& y_2' = a \\
& z_2' = x_2 + z_2^2.
\end{aligned}
$$

The following observation is crucial:

LEMMA 4.2 [Ben90]. *System* (24) *has for $b \neq 0$, real $\lambda_i \neq 0$ explicit solutions $\gamma_i$, $i = 1, 2$ given by*

$$
\begin{aligned}
(25) \qquad & \tilde{x}_2(t) = -\frac{\lambda_i^2}{4} t^2 - \frac{\lambda_i}{2} \\
& \tilde{y}_2(t) = at \\
& \tilde{z}_2(t) = -\frac{\lambda_i}{2} t,
\end{aligned}
$$

where $\lambda_i$, $i = 1, 2$ are the eigenvalues of the linearization of the desingularized flow (12).

*Remark.* In the case $b = 0$ there exists a family of solutions

$$(26) \qquad (\tilde{x}_2(t), \tilde{y}_2(t), \tilde{z}_2(t)) = \left( -\frac{c^2}{4} t^2 - \frac{c}{2}, at + k, -\frac{c}{2} t \right),$$

corresponding to the nonzero eigenvalue $\lambda_1 = c$, with $k \in \mathbb{R}$ since $x_2$ and $z_2$ are decoupled from $y_2$.

These special solutions are algebraic in $t$. The projections of these special solutions into the $(y_2, z_2)$ plane, shown in Fig. 10b, coincide with the eigendirections at the origin of the singular canards shown in Fig. 3. The special solutions $\gamma_i$, $i = 1, 2$ in the folded saddle case are shown in Fig. 10a. Note that to leading order the special solutions satisfy the equation $x_2 + z_2^2 = 0$ as $t \to \pm\infty$.

We will see that the special solutions (25) are backward and forward asymptotic to equilibria $P^-_{\lambda_i}$ and $P^+_{\lambda_i}$, $i = 1, 2$ on the "equator" $\bar{\varepsilon} = 0$ of $\mathbb{S}^3$. The importance of the special solutions $\gamma_i$, $i = 1, 2$ is that they connect the attracting slow manifold across the "upper half" $\bar{\varepsilon} > 0$ of $\mathbb{S}^3$ to the repelling slow manifold or vice versa. To study the unbounded branches of these solutions in forward and backward time we need one additional chart $\kappa_1$ corresponding to a directional blow-up in direction of the negative $x$-axis.
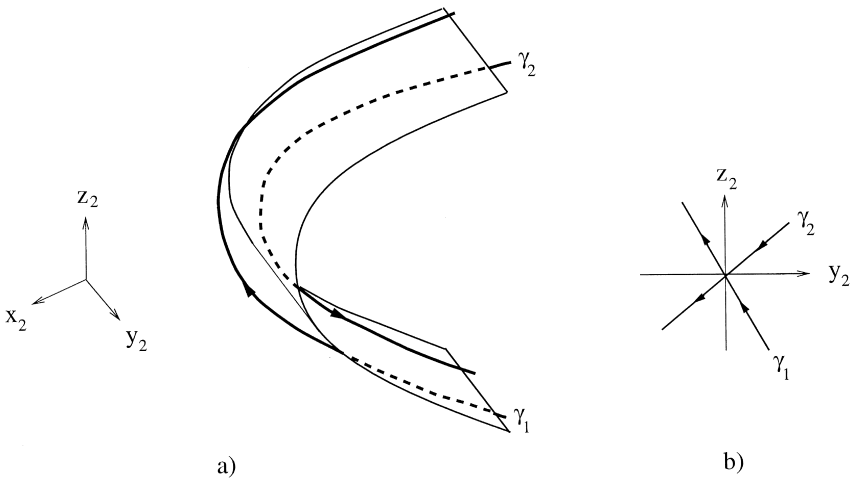


**FIG. 10.** (a) Special solutions in chart $\kappa_2$, $r_2 = 0$; (b) projection in $(y_2, z_2)$ plane.

### 4.2. *Dynamics in Chart $\kappa_1$*

We consider transformation (20) with $\bar{x} = -1$, i.e., we consider the directional blow-up $\Phi_1 : \mathbb{R}^4 \to \mathbb{R}^4$ given by

$$\Phi_1(r_1, y_1, z_1, \varepsilon_1) = (-r_1^2, r_1 y_1, r_1 z_1, r_1^2 \varepsilon_1).$$

After transformation of system (18) and desingularization we obtain

(27)
$$
\begin{aligned}
r_1' &= -\tfrac{1}{2} r_1 \varepsilon_1 g_{11}(r_1, y_1, z_1, \varepsilon_1) \\
y_1' &= \varepsilon_1 \big( g_{12}(r_1, y_1, z_1, \varepsilon_1) + \tfrac{1}{2} y_1 g_{11}(r_1, y_1, z_1, \varepsilon_1) \big) \\
z_1' &= f_1(r_1, y_1, z_1, \varepsilon_1) + \tfrac{1}{2} \varepsilon_1 z_1 g_{11}(r_1, y_1, z_1, \varepsilon_1) \\
\varepsilon_1' &= \varepsilon_1^2 g_{11}(r_1, y_1, z_1, \varepsilon_1),
\end{aligned}
$$

with

$$
\begin{aligned}
g_{11}(r_1, y_1, z_1, \varepsilon_1) &= by_1 + cz_1 + r_1(\beta_1 + \beta_2 \varepsilon_1 + \beta_3 y_1^2 + \beta_4 z_1^2 + \beta_5 y_1 z_1) + O(r_1^2) \\
g_{12}(r_1, y_1, z_1, \varepsilon_1) &= a + r_1(\gamma_1 y_1 + \gamma_2 z_1) + O(r_1^2) \\
f_1(r_1, y_1, z_1, \varepsilon_1) &= -1 + z_1^2 + r_1(\alpha_1 z_1^3 + \alpha_2 y_1 \varepsilon_1 + \alpha_3 z_1 \varepsilon_1) + O(r_1^2).
\end{aligned}
$$

Note that system (27) has two invariant subspaces, namely the hyperplanes $r_1 = 0$ and $\varepsilon_1 = 0$. Their intersection corresponds to the invariant plane $\{(0, y_1, z_1, 0) : (y_1, z_1) \in \mathbb{R}^2\}$. The dynamics in this plane is governed by

$$
\begin{aligned}
y_1' &= 0 \\
z_1' &= -1 + z_1^2.
\end{aligned}
$$

There are two lines of equilibria $L_{a,1} = (0, y_1, -1, 0)$ and $L_{r,1} = (0, y_1, 1, 0)$ which are normally hyperbolic, the nonzero eigenvalue is $-2$ for $L_{a,1}$, and $2$ for $L_{r,1}$. The dynamics in the invariant hyperplane $\varepsilon_1 = 0$ is governed by

$$
\begin{aligned}
r_1' &= 0 \\
y_1' &= 0 \\
z_1' &= -1 + z_1^2 + \alpha_1 z_1^3 r_1 + O(r_1^2).
\end{aligned}
$$

This system has a normally hyperbolic surface $S_{a,1}$ of equilibria emanating from $L_{a,1}$ and a surface $S_{r,1}$ of equilibria emanating from $L_{r,1}$. For $r_1$ small this follows from the implicit function theorem. Along the surface $S_{a,1}$ the

nonzero eigenvalue is negative and close to $-2$ for small $r_1$. Along $S_{r,1}$ the situation is similar, however the nonzero eigenvalue is positive and close to $2$ for small $r_1$. Note that $S_{a,1}$ resp. $S_{r,1}$ corresponds to the attracting resp. repelling branch $S_a$ resp. $S_r$ of the critical manifold. We have gained normal hyperbolicity at the lines $L_{a,1}$ and $L_{r,1}$ due to the blow-up. The dynamics in the invariant hyperplane $\varepsilon_1 = 0$ is shown in Fig. 11.

The dynamics in the invariant hyperplane $r_1 = 0$ is governed by

$$
\begin{aligned}
y_1' &= \varepsilon_1(a + \tfrac{1}{2}\,y_1(by_1 + cz_1)) \\
z_1' &= -1 + z_1^2 + \tfrac{1}{2}\,\varepsilon_1 z_1(by_1 + cz_1) \\
\varepsilon_1' &= \varepsilon_1^2(by_1 + cz_1).
\end{aligned}
$$

We recover the lines of equilibria $L_{a,1}$ and $L_{r,1}$ and one additional zero eigenvalue due to the third equation. Hence, there exist two-dimensional center manifolds $C_{a,1}$, $C_{r,1}$ of the lines $L_{a,1}$, $L_{r,1}$. The flow in $\varepsilon_1$-direction is determined by the sign of $by_1 \pm c$.

LEMMA 4.3. *Points on the lines $L_{a,1/r,1} = (0, y_1, \mp 1, 0)$ with $y_1 \in I \subset \mathbb{R}$ are non-hyperbolic equilibria of (27) with triple eigenvalue zero. The nonzero eigenvalue is given by $\lambda = \mp 2$.*
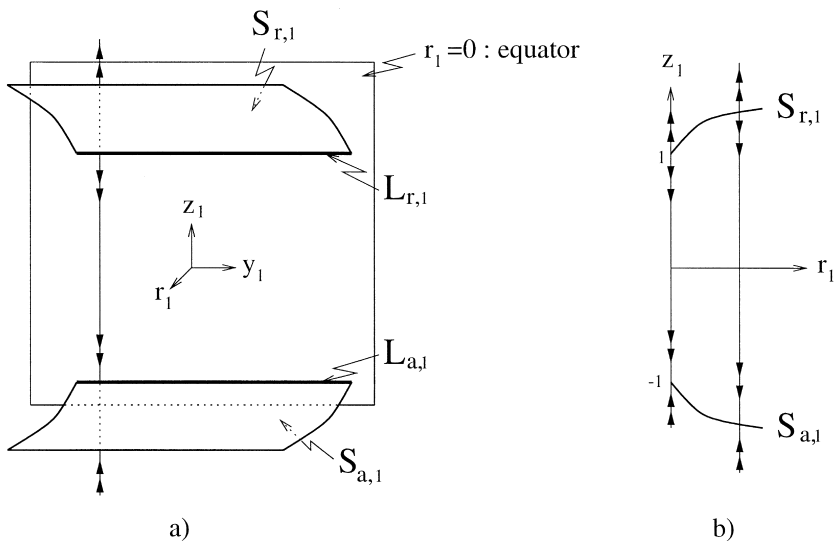


FIG. 11. (a) Dynamics in hyperplane $\varepsilon_1 = 0$ in chart $\kappa_1$; (b) projection in $(r_1, z_1)$ plane.

*Proof.* The linearization of system (27) at an equilibrium $(0, y_1, \pm 1, 0)$ is given by

$$\begin{pmatrix} 0 & 0 & 0 & 0 \\ 0 & 0 & 0 & a+1/2y_1(by_1 \pm c) \\ \pm \alpha_1 & 0 & \pm 2 & \pm 1/2(by_1 \pm c) \\ 0 & 0 & 0 & 0 \end{pmatrix}.$$

The eigensystem of this matrix is shown in Table I, where the last vector is a generalized eigenvector. ∎

We restrict attention to the set

$$D_1 = \{(r_1, y_1, z_1, \varepsilon_1) : 0 \leq r_1 \leq \rho, 0 \leq \varepsilon_1 \leq \delta, |y_1| \leq \sigma\}.$$

PROPOSITION 4.1. *For $\sigma$, $\rho$, and $\delta$ sufficiently small the following assertions hold for system* (27):

(1) *There exists an attracting three dimensional center manifold $M_{a,1}$ of the line of equilibria $L_{a,1} = (0, y_1, -1, 0)$, $y_1 \in I$, containing the surface of equilibria $S_{a,1}$ and the center manifold $C_{a,1}$. In $D_1$ the manifold $M_{a,1}$ is given as a graph $z_1 = h_a(r_1, y_1, \varepsilon_1)$. The branch of $C_{a,1}$ in $r_1 = 0$ is unique for $by_1 - c > 0$.*

(2) *There exists a repelling three dimensional center manifold $M_{r,1}$ of the line of equilibria $L_{r,1} = (0, y_1, 1, 0)$, $y_1 \in I$, containing the surface of equilibria $S_{r,1}$ and the center manifold $C_{r,1}$. In $D_1$ the manifold $M_{r,1}$ is given as a graph $z_1 = h_r(r_1, y_1, \varepsilon_1)$. The branch of $C_{r,1}$ in $r_1 = 0$ is unique for $by_1 + c < 0$.*

(3) *There exists a stable invariant foliation $F_s$ with base $M_{a,1}$ and one-dimensional fibers. For any $k > -2$ there exists a choice of positive $\sigma$, $\rho$ and $\delta$ such that the contraction along $F_s$ is stronger than $e^{kt_1}$.*

TABLE I

Eigensystem in Chart $\kappa_1$

| Eigenvalue | Multiplicity | Eigenvector | Direction |
|---|---|---|---|
| $\pm 2$ | 1 | $(0, 0, 1, 0)$ | $z_1$ |
| 0 | 3 | $(0, 1, 0, 0)$ | $y_1$ |
| | | $(1, 0, -\alpha_1/2, 0)$ | $(r_1, z_1)$ |
| | | $(0, 0, by_1 \pm c, -4)$ | $(z_1, \varepsilon_1)$ |

(4) *There exists an unstable invariant foliation $F_u$ with base $M_{r,1}$ and one-dimensional fibers. For any $k < 2$ there exists a choice of positive $\sigma$, $\rho$ and $\delta$ such that the expansion along $F_u$ is stronger than $e^{kt_1}$.*

*Proof.* These assertions follow from Lemma 4.3 and from invariant manifold theory (see, e.g., [HPS77, Fen79]). ∎

Next we use transformation (21) to rewrite the special solutions (25) from chart $\kappa_2$ in chart $\kappa_1$. A straightforward calculation shows that

$$\kappa_{12}(\gamma_i(t)) = \left( 0, \frac{at}{\sqrt{(1/4)\,\lambda_i^2 t^2 + (1/2)\,\lambda_i}}, \frac{-(1/2)\,\lambda_i t}{\sqrt{(1/4)\,\lambda_i^2 t^2 + (1/2)\,\lambda_i}}, \frac{1}{(1/4)\,\lambda_i^2 t^2 + (1/2)\,\lambda_i} \right),$$

with sufficiently large $|t|$. In the limit $t \to \pm\infty$ we obtain

$$(28) \qquad P_{\lambda_i}^{\pm} = \lim_{t \to \pm\infty} \kappa_{12}(\gamma_i(t)) = \left( 0, \pm\frac{2a}{|\lambda_i|}, \mp sgn(\lambda_i), 0 \right),$$

where $sgn(\lambda_i)$ denotes the sign of the eigenvalue $\lambda_i$. This shows that each of the special orbits from chart $\kappa_2$ emanates from a point on one of the lines of equilibria $L_{a,1/r,1}$ in chart $\kappa_1$ and approaches a point on the other line in chart $\kappa_1$. This explains why we need just the two charts $\kappa_1, \kappa_2$ for the analysis of the dynamics close to the special solutions. Keep in mind that the surfaces of equilibria $S_{a,1/r,1}$ in chart $\kappa_1$ emanating from $L_{a,1/r,1}$ represent the branches of the critical manifold.

PROPOSITION 4.2. *For a special solution $\gamma_i$, $i = 1, 2$ corresponding to a singular canard let $T > 0$ be sufficiently large. Then the part of $\gamma_i(t)$ corresponding to $t \in (-\infty, -T)$ is part of the unique branch of the center-manifold $C_{a,1}$ in $r_1 = 0$, $\varepsilon_1 > 0$ in chart $\kappa_1$. The part of $\gamma_i(t)$ corresponding to $t \in (T, \infty)$ is part of the unique branch of the center-manifold $C_{r,1}$ in $r_1 = 0$, $\varepsilon_1 > 0$.*

*Proof.* According to Lemma 2.3, $\lambda_i < 0$ holds for a singular canard. It follows that equilibria (28) on the line $L_{a,1}$ resp. $L_{r,1}$ satisfy the conditions $by_1 - c > 0$ resp. $by_1 + c < 0$ of Proposition 4.1. Thus, the center manifolds $C_{a,1}$ resp. $C_{r,1}$ are unique at the points $P_{\lambda_i}^{\pm}$ for $\varepsilon_1 > 0$ by Proposition 4.1. Furthermore, the tangent vectors of $\gamma_i$ in chart $\kappa_1$ at the equilibria (28) given by

$$\lim_{t \to \pm\infty} \frac{\dfrac{d}{dt}\kappa_{12}(\gamma_i(t))}{\left\| \dfrac{d}{dt}\kappa_{12}(\gamma_i(t)) \right\|} = (0, \pm 2a, \mp|\lambda_i|, -4)$$

are tangent to the center manifolds $C_{r,1/a,1}$ (see Table I). Note that the generalized eigenvector $(0, 0, by_1 \pm c, -4)$ of Table I is an eigenvector at the equilibrium $P_{\lambda_i}^{\pm}$, $i = 1, 2$. This implies the assertion. ∎

The dynamics in chart $\kappa_1$ near a special solution $\gamma_i$ in the hyperplane $r_1 = 0$ is illustrated in Fig. 12.

*Remark.* Similar calculations show that in the case $b = 0$ the family of special solutions (26) approaches the same point $P_{\lambda_i}^{\pm}$ in chart $\kappa_1$ and Proposition 4.2 holds too. The only difference arises in the calculation of the tangent vectors at the equilibria (28). For $k = 0$ we obtain the same vector as before. All the other special solutions with $k \neq 0$ approach the equilibria tangent to the vector $(0, 1, 0, 0)$; i.e., they are also tangent to the center manifolds $C_{r,1/a,1}$ (see Table I). Note that the special solution with $k = 0$ is unique in chart $\kappa_1$. In the following we will just focus on this special solution (25).

The center manifolds $C_{a,1}$ resp. $C_{r,1}$ can be extended along the special solutions. Thus, the special solutions correspond to the intersection of the
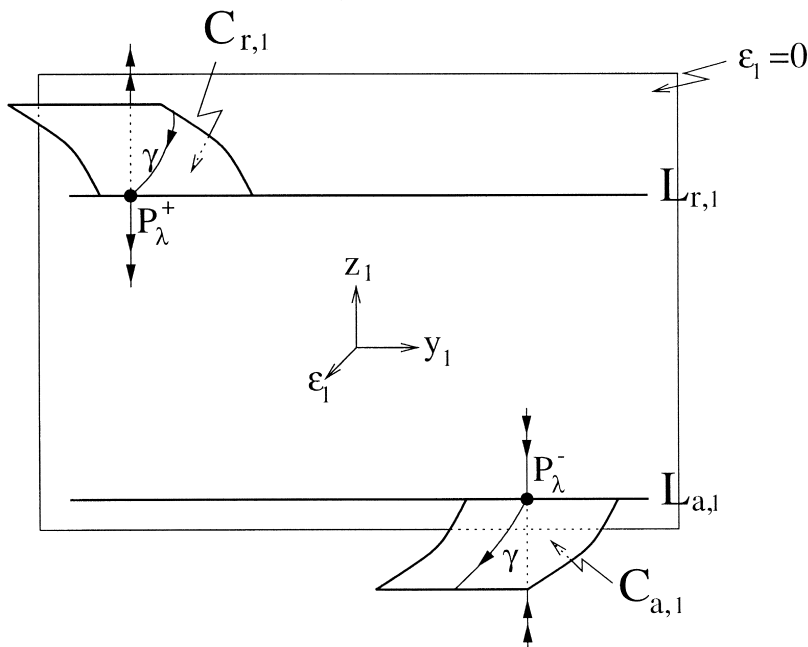


**FIG. 12.** Dynamics near a special solution in chart $\kappa_1$ in hyperplane $r_1 = 0$.

center manifolds $\bar{C}_a$ resp. $\bar{C}_r$ on the sphere $\mathbb{S}^3$. In the next section we want to obtain a transversality condition for this intersection, which implies the persistence of the intersection between the center manifolds $\bar{M}_a$ and $\bar{M}_r$ of the full blown-up problem (18), i.e., the existence of maximal canards.

### 4.3. *Existence of Canards*

For faux canards we obtain a result immediately.

PROPOSITION 4.3. *Assume system* (8). *A singular faux canard implies the existence of a two parameter family of faux canard solutions for sufficiently small* ε.

*Proof.* The special solution corresponding to a singular faux canard starts in a repelling domain and ends in an attracting domain, i.e. we are in a source-sink like scenario. The special solution lies in the non-unique parts of the center manifolds $C_{r,1}$ and $C_{a,1}$ (see Proposition 4.1). Hence, the corresponding center-unstable manifold $W^u(C_{r,1})$ and the center-stable manifold $W^s(C_{a,1})$ of the special solution have a full three-dimensional intersection. Thus, the intersection of the manifolds $W^u(\bar{M}_r)$ and $W^s(\bar{M}_a)$ is full. ∎

For special solutions corresponding to singular canards transversality is not obvious and we will argue by using the variational equation.

PROPOSITION 4.4. *Let* $\gamma_i$ *be a special solution* (25) *corresponding to a singular canard. If* $\dot{\gamma}_i$ *is (up to a multiplicative constant) the only algebraic solution of the variational equation of system* (24) *along* $\gamma_i$, *then the intersection of* $\bar{C}_a$ *and* $\bar{C}_r$ *along* $\gamma_i$ *is transversal.*

*Proof.* We have seen that the special solution emanates from the center manifold $C_{a,1}$ and approaches the center manifold $C_{r,1}$ in the hyperplane $r_1 = 0$ of chart $\kappa_1$, where $C_{a,1}$ is strongly attracting while $C_{r,1}$ is strongly repelling. Thus, solutions of system (24) which are not emanating from $C_{a,1}$ and approaching $C_{r,1}$ are growing exponentially in backward or forward time. The variational equation along $\gamma_i$ acts on the tangent bundles $T_{\gamma_i}\mathbb{R}^3$. The only possibility to obtain solutions of the variational equation which are not growing exponentially are those who are in the intersection of $T_{\gamma_i}C_{a,2}$ and $T_{\gamma_i}C_{r,2}$ in the subspace $r_2 = 0$, where $C_{a,2}$ and $C_{r,2}$ are the extensions of the center manifolds $C_{a,1}$ and $C_{r,1}$ along $\gamma_i$ in chart $\kappa_2$. The solution $\dot{\gamma}_i$ lies always in the intersection of $T_{\gamma_i}C_{a,2}$ and $T_{\gamma_i}C_{r,2}$ by definition. If $\dot{\gamma}_i$ is the only algebraic solution of the variational equation, then the intersection of $T_{\gamma_i}C_{a,2}$ and $T_{\gamma_i}C_{r,2}$ and hence the intersection of $C_{a,2}$ and $C_{r,2}$ is transversal along the special solution (see Fig. 13). ∎
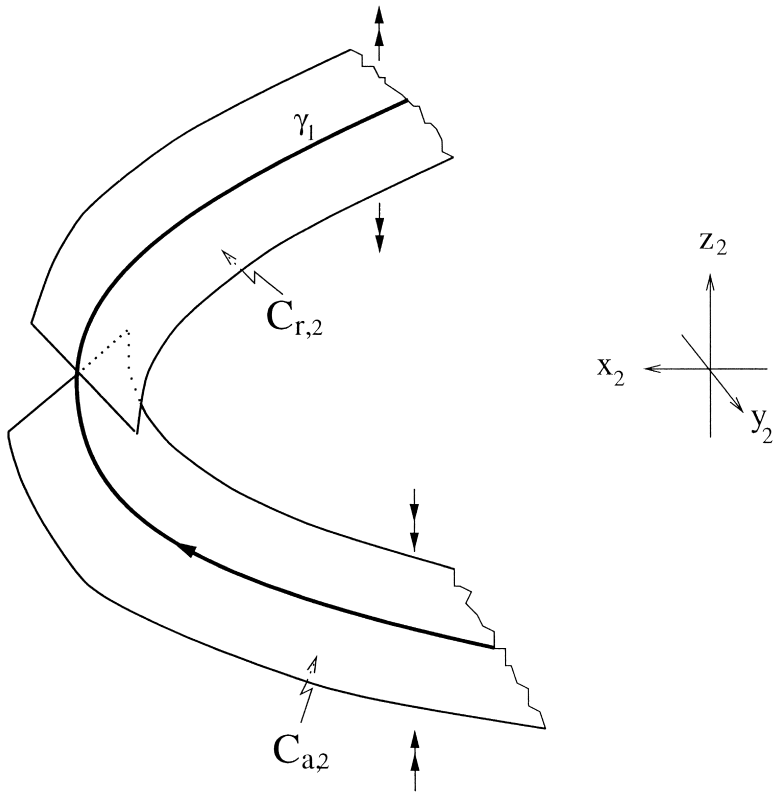
**FIG. 13.** Extensions of center manifolds $C_{a,1}$, $C_{r,1}$ in chart $\kappa_2$.

In the following we derive conditions for transversality. To obtain a better geometrical understanding we first rectify the special solution along the $z_2$-axis. This is done by the coordinate transformation

$$(x_2, y_2, z_2, r_2) \mapsto \left( x_2 + z_2^2 + \frac{\lambda_i}{2}, \, y_2 + \frac{2a}{\lambda_i} z_2, \, z_2, \, r_2 \right).$$

Applying this coordinate transformation to system (23) leads to

$$\tilde{x}_2' = 2\tilde{x}_2 z_2 + b\tilde{y}_2 + r_2(\tilde{h}_1 + 2z_2\tilde{h}_3)$$

$$\tilde{y}_2' = \frac{2a}{\lambda_i} \tilde{x}_2 + r_2 \left( \tilde{h}_2 + \frac{2a}{\lambda_i} \tilde{h}_3 \right)$$

$$z_2' = \tilde{x}_2 - \frac{\lambda_i}{2} + r_2\tilde{h}_3$$

$$r_2' = 0.$$

The special solution (25) is transformed to

$$
\text{(29)} \qquad \tilde{\gamma}_i(t) = \left( 0, 0, -\frac{\lambda_i}{2} t, 0 \right).
$$

The variational equation along $\tilde{\lambda}_i$ is

$$
\text{(30)} \qquad
\begin{aligned}
u' &= -\lambda_i t u + b v \\
v' &= \frac{2a}{\lambda_i} u \\
w' &= u,
\end{aligned}
$$

which can be written for $b \neq 0$, $\lambda_i \neq 0$ as a homogeneous second order differential equation

$$
\text{(31)} \qquad u'' + \lambda_i t u' + \lambda_i (1 - \mu_i)\, u = 0,
$$

with

$$
\mu_i := \frac{\lambda_1 \lambda_2}{\lambda_i^2}.
$$

*Proof of Theorem* 4.1.  Proposition 4.4 implies that the intersection is transversal, iff all solutions of the homogeneous problem (31) grow exponentially in forward or backward time.

Recall by Lemma 2.3 that $\lambda_i < 0$ for singular canards. Hence, we investigate the homogeneous problem (31) just for negative eigenvalues. Keeping this fact in mind, we rescale time by

$$
\text{(32)} \qquad t = \sqrt{\frac{2}{|\lambda_i|}}\; \tau
$$

and obtain the Weber equation

$$
\text{(33)} \qquad \ddot{u} - 2\tau \dot{u} + 2(\mu_i - 1)\, u = 0.
$$

If $\mu_i$ is a natural number, i.e., $\mu_i = n \in \mathbb{N}$, then the polynomial solution $u(\tau)$ of (33) is the Hermite polynomial $H_{n-1}(\tau)$. This solution has $n-1$ alternating zeros in a neighbourhood of $\tau = 0$. For $n-1 < \mu_i < n$ exist two linearly independent solution $u_1(\tau)$ and $u_2(\tau)$ with the property that $u_1(\tau)$ (resp. $u_2(\tau)$) grows algebraically as $\tau \to \infty$ (resp. $\tau \to -\infty$) but grow exponentially as $\tau \to -\infty$ (resp. $\tau \to \infty$). Furthermore, these solutions also posses $n-1$

alternating zeros. Properties of the Weber equation are, e.g., covered in [AS64].

The above calculations and Proposition 4.4 imply that on the sphere $\mathbb{S}^3$, i.e., $\bar{r} = 0$, the center manifolds $\bar{C}_a$ and $\bar{C}_r$ intersect transversally along $\gamma_i$ iff $\mu_i \notin \mathbb{N}$. Since $\bar{C}_a$ and $\bar{C}_r$ are two-dimensional submanifolds of the three-dimensional manifolds $\bar{M}_a$ and $\bar{M}_r$, it follows that $\bar{M}_a$ and $\bar{M}_r$ intersect transversally in a neighbourhood of $\gamma_i$. By blowing down the same holds for $M_a$ and $M_r$. It follows from Proposition 4.1 that the slow manifolds $S_{a,\varepsilon}$ and $S_{r,\varepsilon}$ are exponentially close to $\varepsilon$-sections of $M_a$ and $M_r$. Hence, $S_{a,\varepsilon}$ and $S_{r,\varepsilon}$ intersect in a maximal canard solution.

In the folded saddle scenario we have $\lambda_1 < 0 < \lambda_2$ which implies that $\mu_1 = \lambda_2/\lambda_1$ is negative. Thus, in the folded saddle scenario a singular canard always perturbs to a canard solution for sufficiently small $\varepsilon$.

In the folded node scenario we have $\lambda_1 < \lambda_2 < 0$ which implies that $0 < \mu_1 < 1$ for solutions corresponding to $\lambda_1$ and $1 < \mu_2$ for solutions corresponding to $\lambda_2$. Hence, in the folded node scenario a canard solution corresponding to the stronger eigenvalue $\lambda_1$ exists for sufficiently small $\varepsilon$. A canard solution corresponding to the weaker eigenvalue $\lambda_2$ exists, if $\lambda_1/\lambda_2 \notin \mathbb{N}$ is not a natural number.  ∎

The geometrical meaning of the parameter $\mu_2$ is described in the following

LEMMA 4.4. *Suppose we are in the node scenario and that $n-1 < \mu_2 < n$ holds for the special solution $\lambda_2$. Then the slow manifolds $S_{a,\varepsilon}$ and $S_{r,\varepsilon}$ twist $n-1$ times around the corresponding maximal canard solution in the neighbourhood of the fold-curve.*

*Proof.* The solutions $(u(t), v(t))$ of system (30) correspond to the transversal directions along $\tilde{\gamma}_2(t)$ of the tangent bundle $T_{\tilde{\gamma}_2}(t)\, \bar{C}_{a,2}$ resp. $T_{\tilde{\gamma}_2(t)}\, \bar{C}_{r,2}$. Thus, the quotient $u(t)\, v^{-1}(t) = \tan\varphi(t)$ corresponds to the rotation angle $\varphi(t)$ of the tangent bundles along the special solution. We substitute

$$\frac{u}{v} = \frac{\lambda_2}{2a} \frac{\psi'}{\psi}$$

and rescale time by (32) to obtain again the Weber equation

$$(34) \qquad\qquad \ddot{\psi} - 2\tau\dot{\psi} + 2\mu_2\psi = 0.$$

For $n-1 < \mu_2 \leqslant n$ all nontrivial solutions $\psi(\tau)$ of (34) posses $n$ alternating zeros in the neighbourhood of the origin. Thus, $v(t)$ has $n$ zeros which correspond to $n$ poles of $\tan\varphi(t)$. Hence, the rotation angle $\varphi(t)$ is

$\pi/2 + (n-1) \cdot \pi$. This corresponds to $n-1$ twists of each tangent bundle $T_{\tilde{\gamma}_2(t)} \bar{C}_{a,2}$ resp. $T_{\tilde{\gamma}_2(t)} C_{r,2}$ around the special solution $\tilde{\gamma}_2$. The twisting-number is an invariant geometric property and holds also for $T_{\lambda_2(t)} C_{a,2}$ resp. $T_{\lambda_2(t)} C_{r,2}$. In the case $n-1 < \mu_2 < n$ the corresponding center manifolds $C_{a,2}$ and $C_{r,2}$ intersect transversally. At a resonance, i.e., $\mu_2 = n \in \mathbb{N}$, the tangent bundles of the corresponding center manifolds match up, i.e., $T_{\lambda_2(t)} C_{a,2} = T_{\lambda_2(t)} C_{r,2}$ for all $t$, forming a single band with $n$ twists. In this case the intersection of the corresponding center manifolds $C_{a,2}$ and $C_{r,2}$ is not transversal. When $\mu_2$ is passing through a resonance the number of zeros of solutions $u(t)$ and $v(t)$ changes by unity and this leads to one more twisting of the band. For another description of this geometric property we refer to [Ben90, MKKR94]. ∎

The next results concern the degenerate scenarios.

PROPOSITION 4.5. *In the folded node scenario of system* (8) *all resonances $\mu_2 \in \mathbb{N}$ can be realized by variation of the parameter b.*

*Proof.* The eigenvalues in the folded node scenario are $\lambda_{1,2} = ((c \mp \sqrt{c^2 - 8ab})/2$ with $0 < 8ab < c^2$. A resonance occurs for $\lambda_1/\lambda_2 \in \mathbb{N}$. The limit $\lim_{b \to 0+} \lambda_1/\lambda_2 = \infty$ gives the folded saddle-node scenario for the zero eigenvalue. The limit $\lim_{b \to c^2/8a-} \lambda_1/\lambda_2 = 1$ gives the folded degenerate node scenario. Thus, all resonances occur since the term $\lambda_1/\lambda_2$ as a function of $b$ is strictly decreasing for $b \in (0, c^2/8a)$. ∎

We have no result in the folded degenerate node scenario of system (8) since for $\mu = 1$ transversality is violated. Hence, we do not know if canards exist in this case.

The derivation of the Weber equation holds only for $b \neq 0$, $\lambda_i \neq 0$. Thus, we obtain for $\mu_1 = 0$, i.e., in the folded saddle-node case with $(a = 0, b \neq 0)$, that the corresponding Weber equation (33) has only solutions with exponential growth.

PROPOSITION 4.6. *In the folded saddle-node scenario of system* (8) *with* $(a = 0, b \neq 0)$ *a singular canard corresponding to the nonzero eigenvalue $\lambda_1 = c < 0$ of the linearization of the desingularized flow* (12) *always perturbs to a canard solution for sufficiently small $\varepsilon$.*

In the other scenario $(a \neq 0, b = 0)$ of the folded saddle-node case we see immediately that the variational equation (30) has a family of bounded solutions which is due to the existence of the family of special solutions (26); i.e., the existence of canards cannot be shown by means of transversality for $r_2 = 0$.

*Remark.* Our transversality argument was based on the variational equation along special solutions in the unperturbed subspace $r_2 = 0$ in chart $\kappa_2$; i.e., we did not use the information of the perturbation. Measuring the distances of the center manifolds $\bar{M}_a$ and $\bar{M}_r$ along the special solutions in the whole blown-up system allows to analyse the non-transversal cases. This is done by a Melnikov-type argument on unbounded domains in chart $\kappa_2$. The bifurcation analysis of canards in the resonant folded node cases and in the subcase ($a \neq 0$, $b = 0$) of the folded saddle-node based on these ideas will be the topic of another publication. We expect that these bifurcations are important for the global, dynamics of systems like the forced van der Pol oscillator (15).

# REFERENCES

[AS64]   M. Abramowitz and A. Stegun, "Handbook of Mathematical Functions," National Bureau of Standards Applied Mathematics Series, Vol. 55, Natl. Bur. of Standards, Washington, DC, 1964.

[BCDD81] E. Benoit, J. F. Callot, F. Diener, and M. Diener, Chasse au canard, *Collect. Math.* **31–32**, Nos. 1–3 (1981), 37–119.

[Ben83]  E. Benoit, Systèmes lents-rapides dans $R^3$ et leurs canards, *Asterisque* **109–110** (1983), 159–191.

[Ben90]  E. Benoit, Canards et enlacements, *Publ. Inst. Hautes Études Sci.* **72** (1990), 63–91.

[Bra93]  B. Braaksma, "Critical Phenomena in Dynamical Systems of van der Pol Type," Thesis, Rijksuniversiteit te Utrecht, The Netherlands, 1993.

[BM90]   M. Brunella and M. Miari, Topological equivalence of a plane vector field with its principal part defined through Newton polyhedra, *J. Differential Equations* **85** (1990), 338–366.

[Bru80]  A. D. Bruno, "Local Methods in Nonlinear Differential Equations," Springer-Verlag, Berlin/New York, 1980.

[DR91]   Z. Denkowska and R. Roussarie, A method of desingularization for analytic two-dimensional vector field families, *Bol. Soc. Bras. Mat.* **22**, No. 1 (1991), 93–126.

[Die84]  M. Diener, The canard unchained or how fast/slow dynamical problems bifurcate, *Math. Intelligence* **6** (1984), 38–49.

[Die94]  M. Diener, Regularizing microscopes and rivers, *SIAM J. Appl. Math.* **25** (1994), 148–173.

[Dum91]  F. Dumortier, Local study of planar vector fields: Singularities and their unfoldings, *in* "Structures in Dynamics, Finite Dimensional Deterministic Studies" (H. W. Broer *et al.*, Eds.), Stud. Math. Phys., Vol. 2, pp. 161–241, North-Holland, Amsterdam, 1991.

[Dum93]  F. Dumortier, Techniques in the theory of local Bifurcations: Blow up, normal forms, nilpotent bifurcations, singular perturbations, *in* "Bifurcations and Periodic Orbits of Vector Fields" (D. Szlomiuk, Ed.), pp. 19–73, Kluwer Academic, Dordrecht, 1993.

[DR96]   F. Dumortier and R. Roussarie, Canard cycles and center manifolds, *Mem. Amer. Math. Soc.* **557** (1996).

[Eck83]   W. Eckhaus, Relaxation oscillations including a standard chase on French ducks, *in* "Asymptotic Analysis, II," Lecture Notes in Math., Vol. 985, pp. 449–494, Springer-Verlag, New York/Berlin, 1983.

[Fen71]   N. Fenichel, Persistence and smoothness of invariant manifolds and flows, *Indiana Univ. Math. J.* **21** (1971), 193–226.

[Fen79]   N. Fenichel, Geometric singular perturbation theory, *Differential Equations* **31** (1979), 53–98.

[GH83]   J. Guckenheimer and P. Holmes, "Nonlinear Oscillations, Dynamical Systems and Bifurcations of Vector Fields," Applied Mathematical Sciences, Vol. 42, Springer-Verlag, New York, 1983.

[HPS77]   M. W. Hirsch, C. C. Pugh, and M. Shub, "Invariant Manifolds," Lecture Notes in Mathematics, Vol. 583, Springer-Verlag, New York, 1977.

[Jon95]   C. K. R. T. Jones, Geometric singular perturbation theory, *in* "Dynamical Systems," Lecture Notes in Math., Vol. 1609, pp. 44–120, Springer-Verlag, New York/Berlin, 1995.

[KS01a]   M. Krupa and P. Szmolyan, Geometric analysis of the singularly perturbed planar fold, *in* Multiple Time Scales Dynamical Systems, IMA Volumes in Mathematics and Its Applications, Vol. 122, pp. 89–116, Springer-Verlag, New York/Berlin, 2001.

[KS01b]   M. Krupa and P. Szmolyan, Extending geometric singular perturbation theory to nonhyperbolic points - fold and canard points in two dimensions, *SIAM J. Math. Anal.* **33**, No. 2 (2001), 286–314.

[KS01c]   M. Krupa and P. Szmolyan, Relaxation oscillations and canard explosion, *J. Differential Equations* **174**, No. 2 (2001), 312–368.

[KS01d]   M. Krupa and P. Szmolyan, Extending slow manifolds near transcritical and pitchfork sungularities, *Nonlinearity*, in press.

[MS01]   A. Milik and P. Szmolyan, Multiple time scales and canards in a chemical oscillator, *in* Multiple Time Scales Dynamical Systems, IMA Volumes in Mathematics and Its Applications, Vol. 122, pp. 117–140, Springer-Verlag, New York/Berlin, 2001.

[MR80]   E. F. Mishchenko and N. Kh. Rozov, "Differential Equations with Small Parameters and Relaxation Oscillations," Plenum, New York, 1980.

[MKKR94] E. F. Mishchenko, Yu. S. Kolesov, A. Yu. Kolesov, and N. Kh. Rhozov, "Asymptotic Methods in Singularly Perturbed Systems," Monographs in Contemporary Mathematics, Consultants Bureau, New York, 1994.

[Rou93]   R. Roussarie, Techniques in the theory of local bifurcations: Cyclicity and desingularization, *in* "Bifurcations and Periodic Orbits of Vector Fields" (D. Szlomiuk, Ed.), pp. 347–382, Kluwer Academic, Dordrecht, 1993.

[Wec98]   M. Wechselberger, "Singularly Perturbed Folds and Canards in $\mathbb{R}^3$," thesis, Vienna University of Technology, Austria, 1998.